

Hydrogen-related defects in hydrogenated amorphous semiconductors

Shu Jin* and Lothar Ley

Universität Erlangen, Institut für Technische Physik, Erwin-Rommel-Strasse 1, D-8520 Erlangen, Federal Republic of Germany

(Received 2 January 1991)

One of the key steps in the formation of glow-discharge-deposited (GD) *a*-Si:H or *a*-Ge:H films by plasma deposition from the gas phase is the elimination of excess hydrogen from the growth surface which is necessary for the cross linking of the Si or Ge network and the reduction of the defect density associated with the hydrogen-rich surface layer. The high defect density ($\sim 10^{18} \text{ cm}^{-3}$) in a growing surface layer can, depending on preparation conditions, be either reduced (to $\sim 10^{16} \text{ cm}^{-3}$) or be trapped in the bulk upon subsequent growth, as evidenced by a great deal of data. However, little is known about its origin and implication. We have investigated the change in electronic structure related with this process using UHV-evaporated *a*-Ge as a model system, subjected to thermal hydrogenation, plasma hydrogenation, and various annealing cycles. The density of occupied states in the pseudogap of the *a*-Ge:(H) surface (probing depth $\sim 50 \text{ \AA}$) was determined with total-yield photoelectron spectroscopy. In this way, effects of thermal annealing, hydrogenation, and ion bombarding on the near-surface defect density could be studied. We identify in room-temperature (RT) hydrogenated *a*-Ge:H another defect at about $E_v + 0.45 \text{ eV}$ in addition to the dangling-bond defect. This defect exists at the initial stage of hydrogen incorporation, decreases upon $\sim 250^\circ\text{C}$ annealing, and is restored upon RT rehydrogenation. Therefore we suspect that this defect is hydrogen induced and concomitant with the formation of unexpected bondings [both multiply bonded XH_x ($X = \text{Si or Ge and } x = 2 \text{ and } 3$) and polyhydride $(XH_2)_n$ configurations] favored at RT hydrogenation. As a possible candidate we suggest the Ge-H-Ge three-center bond in which one electron is placed in a nonbonding orbital that gives rise to the paramagnetic state in the gap of *a*-Ge:H observed here. This defect also accounts for the large defect density at the growing surface in the optimized plasma chemical-vapor-deposition process, where the special bonding configurations mentioned above are the predominant species. The formation and annealing of this defect will be discussed.

I. INTRODUCTION

A minimum of about 5–10 at. % bonded hydrogen is needed to lower the density of deep defects in amorphous silicon or germanium (*a*-Si, *a*-Ge) (Refs. 1 and 2) from $\sim 10^{19} - 10^{20} \text{ cm}^{-3}$ to an astounding $\sim 10^{15} - 10^{16} \text{ cm}^{-3}$. These numbers refer to the densities of spins that are associated with what is accepted to be the principal deep defect in these materials: the Si or Ge “dangling bond” which in its neutral state is occupied by a single electron. Pairing of these electrons with the electron in the hydrogen $1s$ state, i.e., the formation of Si—H, viz., Ge—H bonds is thought to be primarily responsible for the reduction in spin density. Because the corresponding bonding and antibonding states lie outside of the pseudogap of *a*-Si:H and *a*-Ge:H, this “passivation” leads to a concomitant reduction in deep defect states. Driving the hydrogen out of the *a*-Si:H or *a*-Ge:H samples by annealing at sufficiently high temperatures restores the defect density irreversibly to nearly its original value.³ It is thus clear that a minimum concentration of bonded hydrogen is a necessary condition for amorphous Si and Ge of good electronic quality.

But this condition is *far* from sufficient. In fact, samples produced at room temperature with hydrogen concentrations in excess of 30 at. % have usually spin densities^{1,3} exceeding 10^{18} cm^{-3} . Only after annealing at temperatures between 200°C and 250°C does the defect den-

sity reach the low values mentioned above.⁴ The annealing is also accompanied by a decrease in the concentration of bonded hydrogen such that hydrogen evolves preferentially from the multiply bonded SiH_x , viz., GeH_x ($x = 2, 3$) and the polyhydride $[(\text{SiH}_2)_n, (\text{GeH}_2)_n]$ configurations while monohydride species remain. Despite differences in detail this general relationship between hydrogen content, hydrogen configuration, temperature, and defect density holds in published data^{5,6} except for films prepared by homogeneous chemical vapor deposition (HOMOCVD) and Si_2H_6 plasma deposition.⁷ It appears that the high defect density of the nonannealed films is directly or indirectly linked to a high concentration of polyhydride configurations. We shall use the term “polyhydride” in the following loosely to indicate all bonding configurations in which more than one hydrogen atom is bonded to Si or Ge.

In the commonly employed plasma chemical-vapor-deposition (CVD) process for the preparation of *a*-Si:H based devices from SiH_4 , hydrogen incorporation and annealing is performed simultaneously by working at a substrate temperature of about $200^\circ\text{C} - 250^\circ\text{C}$, yielding material of the lowest available defect density. The relationship between defect density and polyhydride configurations would therefore be of purely academic interest were it not for mounting evidence that the surface of these films has a higher defect concentration than the bulk of the material. Ast and Brodsky⁸ showed this difference between surface and bulk in *a*-Si:H; they found

an increase in the activation energy of phosphorus-doped a -Si:H when the film thickness dropped below $0.5 \mu\text{m}$. The analysis of subgap optical absorption in a -Si:H by photothermal deflection spectroscopy (PDS) (Ref. 9) leads to the conclusion that there exist more defects in the surface or interface layer ($2.5 \times 10^{18} \text{ cm}^{-3}$) than in the bulk [$(2-3) \times 10^{15} \text{ cm}^{-3}$]. From photoemission study it has been concluded that the growth surface of a -Si:H (Refs. 10 and 11) and a -Ge:H (Ref. 10) is rich in polyhydrides for deposition or annealing temperatures up to $\sim 300^\circ\text{C}$; only upon annealing to about 350°C are the monohydrides the dominant species in a surface layer about $5-10 \text{ \AA}$ thick.¹⁰ Electronic and structural properties of the growing surface layer can be directly obtained, respectively, from total-yield photoelectron spectroscopy and electron-energy-loss spectroscopy (EELS). Total-yield measurements^{12,13} of a -Si:H and its alloys derive a high-surface defect density ($\sim 10^{18} \text{ cm}^{-3}$) with a sampling depth of $\sim 50 \text{ \AA}$ while EELS (Ref. 14) confirms polyhydrides as the predominant species in the surface layer. Most recently, a detailed and interesting analysis has been done by Hata *et al.* (Ref. 15) of thickness-dependent subgap optical absorption on a -Si:H samples by PDS. They fit defect densities of films spanning over four orders of magnitudes in thickness by assuming that a high defect density ($4 \times 10^{17} \text{ cm}^{-3}$) at the growing surface decays into the bulk due to a thermal annealing process that takes place during film growth. However, no comments have been made with regard to the origin of the high-surface defect density. As indicated above, the high-surface defect density is concomitant with polyhydride configurations and the reduction of the former is thermally activated with an activation energy ($\sim 1 \text{ eV}$) that is comparable to that related to hydrogen motion.¹⁶ Therefore a study of the nature and the origin of these surface defects might help shed some light on the relationship between growth process and defect density and defect distribution in amorphous hydrogenated materials.

Posthydrogenation has been used extensively by Kaplan and co-workers¹⁷ to incorporate controlled and varying amounts of hydrogen into an a -Si film and follow the related variations in electronic properties and structure. Here we employ this method to study the near-surface electronic properties of a -Ge by total yield as a function of hydrogen exposure under different conditions. This approach has a number of advantages compared with a study of a -Ge:H prepared directly by plasma CVD. First, the effect of different hydrogen configurations can be studied on a material that has a definite morphology to start with. Secondly, we can separate the effect of annealing alone on the electronic structure of amorphous materials from the effect of hydrogenation and simultaneous annealing. Third, by comparing plasma hydrogenation with thermal hydrogenation (to be explained below) we distinguish between hydrogen and ion bombardment-induced defects. The utilization of a rather surface sensitive probe (sampling depth $\sim 50-100 \text{ \AA}$), finally, avoids all problems related to a hydrogen concentration gradient in the sample.

The choice of a -Ge rather than a -Si was dictated by experimental considerations such as a lower evaporation

temperature and a reduced reactivity with oxygen. We feel, however, that our results pertain just as well to a -Si and we will use the analogy between the two materials freely in what follows.

In Sec. II we describe experimental details which include sample preparation, yield spectrum, and Fermi-level measurements. We then present in Sec. III the results which indicate a defect in hydrogenated amorphous materials other than the dangling-bond defect. In Sec. IV we discuss its origin and implications. Finally, we conclude our study in Sec. V.

II. EXPERIMENT

Film evaporation, thermal and plasma hydrogenation, yield spectrum, and work-function measurements were all performed in three interconnected UHV chambers with a base pressure of $\sim 10^{-10}$ Torr. Amorphous Ge film with a thickness of $\sim 1000 \text{ \AA}$ was thermally evaporated from fully outgassed single crystalline Ge pieces onto polished stainless steel substrates kept at room temperature (RT). The evaporation rate was monitored with a quartz oscillator and kept at $10 \text{ \AA}/\text{sec}$. Hydrogenation was performed in a rf H_2 plasma (20 W); hydrogen flow and pressure were 5 sccm (where sccm denotes cubic centimeters per minute at STP) and 0.6 mbar, respectively. During or after hydrogenation the sample temperature T_S could be varied between RT and 320°C . The samples were transferred immediately after hydrogenation or annealing from the heater to another sample holder where they were left to cool down to RT *in vacuo*. In this way the sample reached a temperature below 50°C within about 10 min. Thermal hydrogenation was performed by exposing a -Ge to activated hydrogen, i.e., by dosing with H_2 in the presence of a hot filament.

The work function of the samples was measured by determining the contact potential difference (CPD) with respect to an "aged" molybdenum reed using the Kelvin method.¹⁸ The work function of the Mo probe is obtained by adding the CPD of a freshly deposited Au film to its work function ($5.27 \pm 0.02 \text{ eV}$) derived by fitting a Fowler plot¹⁹ to the photoelectric yield spectrum of the film. In the course of this work the Mo work function was calibrated several times and found to have been stable at $4.04 \pm 0.02 \text{ eV}$. This error sets the absolute accuracy of Fermi-level measurements since the Kelvin probe technique allows a much more accurate determination ($\pm 2 \text{ meV}$) of the CPD.

The photoelectric yield $Y(\hbar\omega)$ is defined as the number of electrons emitted into vacuum per incident photon of energy $\hbar\omega$. In amorphous solids $Y(\hbar\omega)$ is given by the following formula:¹²

$$Y(\hbar\omega) \propto \hbar\omega |R(\hbar\omega)|^2 \int_{E_{\text{vac}}}^{\infty} g_v(E - \hbar\omega) g_c(E) dE, \quad (1)$$

where g_v is the initial occupied density of states (DOS), g_c the final DOS, and $R(\hbar\omega)$ the optical-dipole matrix element. It is easy to derive the occupied DOS from $Y(\hbar\omega)$ because of the structureless distribution of g_c above the vacuum level, E_{vac} and the well known energy dependence of $R(\hbar\omega)$.^{12,20}

$$g_v \propto (\hbar\omega)^4 [4Y(\hbar\omega)/\hbar\omega + dY(\hbar\omega)/d(\hbar\omega)]. \quad (2)$$

To agree with conventional photoemission results, we normalize the occupied DOS to a value of 10^{22} states/eV cm⁻³ at the energy 6.2 eV below E_{vac} .¹² The extrapolation of a linear plot of g_v to zero is defined as the top of valence band E_v (refer to Fig. 4 in Ref. 12). For g_v distributions with clearly exponential valence-band tail one can calculate the characteristic energy E_{0v} defined by

$$E_{0v} = 1/\{d[\ln g_v(E)]/dE\}. \quad (3)$$

The probe depth (50–100 Å) of total-yield spectroscopy is limited simultaneously by the depths of photon absorption and photoelectron escape. More experimental details are given elsewhere.¹²

III. RESULTS

Figure 1 shows yield spectra of one *a*-Ge film before and after hydrogenation at temperatures T_S between RT and 320°C for one hour. The position of E_f is marked by vertical lines in the spectra. The top of the valence band E_v was determined for each spectrum as described above and the energies E_f , E_v (referred to the vacuum level), and $E_v - E_f$ are summarized in Fig. 2.

The yield spectrum of as-deposited *a*-Ge is rather structureless and agrees with an early spectrum of *a*-Ge by Ribbing, Pierce, and Spicer²¹ in the range between 5.0 and 6.2 eV where both measurements overlap. The top of the valence band lies at 5.15 eV and the spectrum drops off towards E_f rather steeply. This spectral shape corresponds to a density of states where a large density of de-

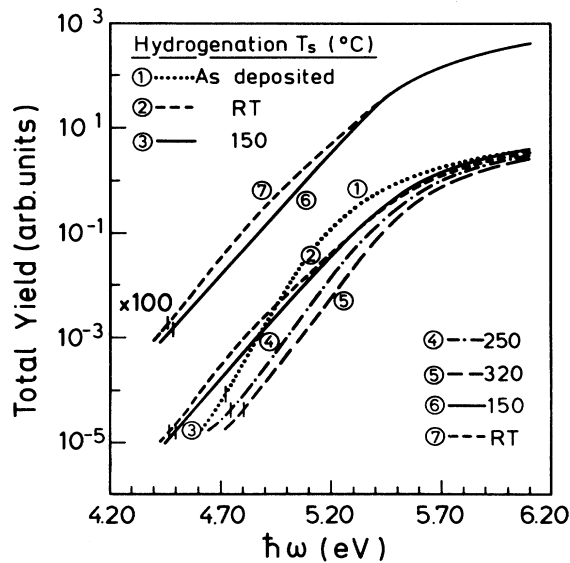


FIG. 1. Yield spectra of *a*-Ge and *a*-Ge:H hydrogenated at various T_S . The vertical marks in the low-energy region indicate the position of E_f as obtained by the Kelvin method. All measurements were carried out on one film upon hydrogenation at different T_S ; the curve numbers also represent the experimental sequence.

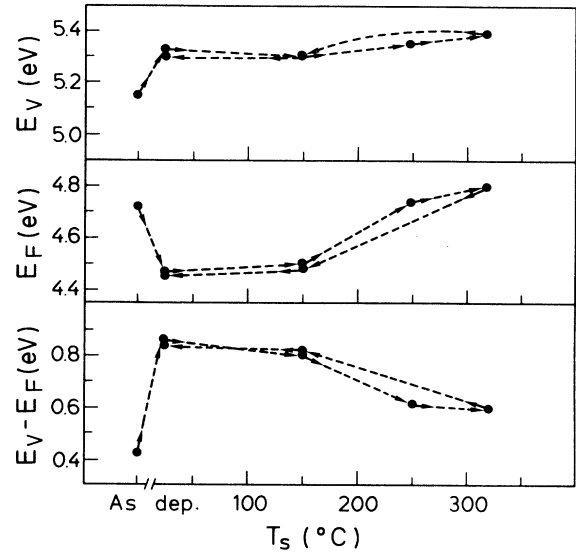


FIG. 2. E_v , E_f , and $E_v - E_f$ as a function of hydrogenation substrate temperature T_S , extracted from the spectra in Fig. 1. E_v refers to the top of valence bands as defined in the text. Both E_f and E_v are measured with respect to vacuum level.

fect states merges into the valence band and the surprisingly steep tailing towards E_f represents the decrease in the defect density rather than the usual exponential valence-band tail that is clearly seen in GD *a*-Ge:H.¹³ We mention in passing that the optical-absorption spectra of *a*-Ge in general²² and also of our film exhibit considerable tailing extending down to midgap energies with a characteristic slope of about 150 meV.

Hydrogenation at RT and 150°C (spectra 2 and 3 in Fig. 1) leads to a significant reduction in the density of states near the top of valence band which results in a recession of E_v by about 0.2 eV (compare Fig. 2). The recession of the valence band with hydrogenation is a commonly observed phenomenon in *a*-Si and *a*-Ge (Ref. 23) and corresponds to the replacement of the weak Ge—Ge bonds by stronger Ge—H bonds. Hydrogenation also reduces the number of the defects within 0.2 eV of the valence-band maximum in *a*-Ge by a factor of 4.

At the same time we observe an increase in the yield around $h\nu=4.8$ eV which corresponds to a hydrogen-induced extra defect density of states at $E_v+0.45$ eV. These defect states push the Fermi level up (toward lower photon energy) by 0.25 eV to a position 0.85 eV above E_v (see Fig. 2).

The defect states disappear for hydrogenation above 200°C and the top of the valence band recedes further (compare spectra 4 and 5 of Fig. 1) up to 5.4 eV below vacuum level. The further reduction in defect density is accompanied by an increase in the work function such that E_f is now about 0.1 eV below its position in unhydrogenated *a*-Ge. Remarkably, the high defect density is fully restored when the same film is rehydrogenated at 150°C and RT, respectively, as is illustrated by spectra 6

and 7 of Fig. 1. They are in fact identical to the corresponding spectra 3 and 2.

The changes in the yield spectra upon hydrogenation at different temperatures are a genuine effect of atomic hydrogen and not due to the annealing of *a*-Ge by the reconstruction of the network. This was confirmed by taking spectra of *a*-Ge films annealed up to 350°C which showed no significant change compared to the ones seen upon hydrogenation; exposure to H₂ (without plasma) had also no effect on the yield spectrum as illustrated in the spectrum of Fig. 3. In the same figure we present the result of a detailed annealing study of an *a*-Ge:H film that was hydrogenated at RT for 10 min (spectrum 2 of Fig. 3). The extra defect signal at $h\nu=4.8$ eV is seen to be reduced progressively as the film is subjected to 30 min isochronal annealing steps of 200°C, 250°C, and 300°C, respectively. With the reduction in the $E_v+0.45$ eV defect band the Fermi level moves closer to E_v as shown in Fig. 4. This figure contains also data points for a 100°C annealing step which has no measurable effect on the yield spectrum.

After a 30 min rehydrogenation at RT (spectrum 6 of Fig. 3) the film is apparently in a state which is indistinguishable from that resulting from the first hydrogenation. This applies, in particular, to the restoring of the defect band at $E_v+0.45$ eV.

In Fig. 5 we present selected densities of occupied states as observed from the yield spectra. Also shown for comparison is the occupied density of states of a GD *a*-Ge:H sample taken from Ref. 13. The defect band has been extracted by subtracting an exponential valence-band tail as indicated in the figure. The valence-band

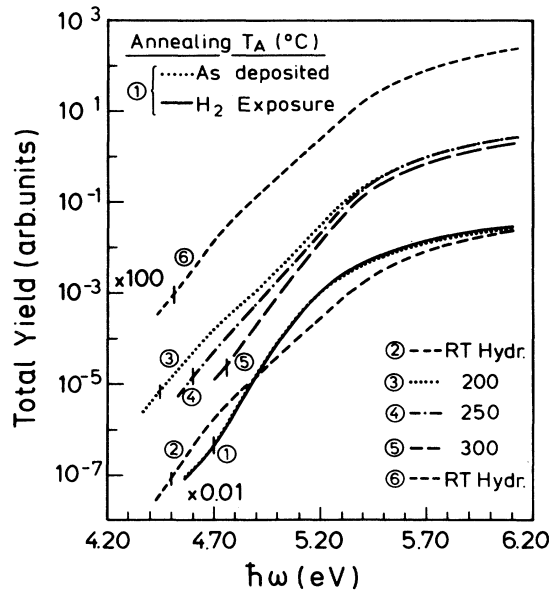


FIG. 3. Yield spectra of *a*-Ge before and after H₂ exposure (curve 1), RT hydrogenated *a*-Ge:H before and after 30 min isochronal annealing at various T_A (curves 2, 3, 4, and 5), and rehydrogenated *a*-Ge:H upon annealing (curve 6). Others are the same as in Fig. 1.

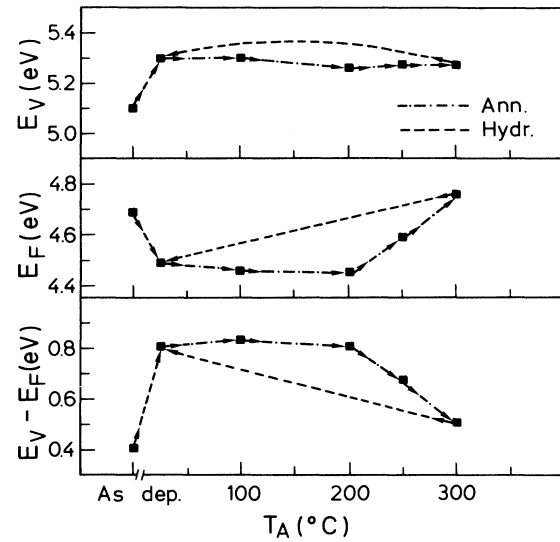


FIG. 4. E_v , E_f , and $E_v - E_f$ as a function of annealing temperature T_A , extracted from the curves in Fig. 3. The dash and dash-dotted lines represent hydrogenation and annealing processes, respectively. Others are the same as in Fig. 2.

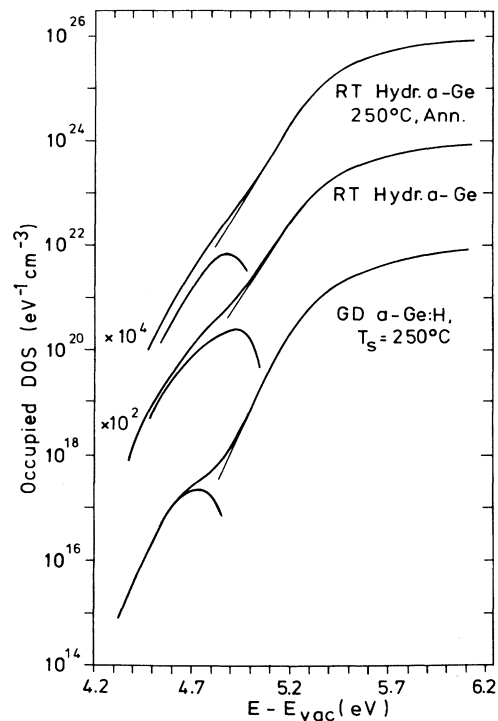


FIG. 5. Occupied density of states of RT hydrogenated *a*-Ge:H before and after 250°C annealing, extracted from the measured yield spectra of Fig. 3. The defect band centered around 4.8 eV has been obtained by subtracting the exponential portion of the valence-band tail from the spectrum. For comparison a spectrum of GD *a*-Ge:H taken from Ref. 13 is also shown.

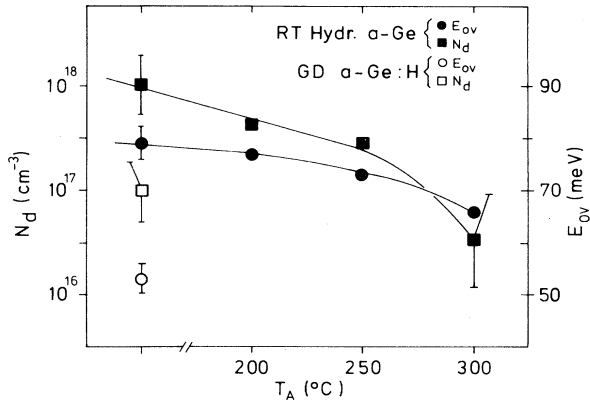


FIG. 6. Defect densities and valence-band tail slopes as a function of annealing temperature. Also shown are the values of GD a -Ge:H. The large defect density ($\sim 10^{17} \text{ cm}^{-3}$) of GD a -Ge:H is due to a highly defective surface layer while the steep valence-band tail ($\sim 53 \text{ meV}$) is dominated by the contribution from the subsurface layers.

slopes E_{0v} and the densities of near surface defect states N_d deduced from the measured yield spectra in the annealing study are summarized in Fig. 6. The slope of the valence-band tail decreases from 80 to 65 meV as the RT hydrogenated a -Ge sample is annealed up to 300°C and the defect density decreases at the same time from $\sim 10^{18} \text{ cm}^{-3}$ to less than $\sim 10^{17} \text{ cm}^{-3}$. This last value has a large uncertainty because the corresponding yield spectrum does not allow a clear distinction between defect band and valence-band tail. The position of the defect level remains at $E_v + 0.45 (\pm 0.05) \text{ eV}$.

IV. DISCUSSION

A. Hydrogen-induced defect

The change in the yield spectrum of a -Ge upon RT hydrogenation mainly consists of a structure due to deep defects which disappears upon annealing above 250°C. The structure is not present when the sample is hydrogenated at 250°C or above. Moreover this process appears to be reversed when the sample is subjected to a renewed plasma hydrogenation at RT. Therefore one naturally asks whether the hydrogen-induced defects are the same as the dangling bonds widely discussed as main defects in these materials.

We argue that the hydrogen-induced-defect band that appears 0.45 eV above E_v is due to polyhydride configurations. We first have to ascertain that these defects are different from the dangling bonds present in unhydrogenated Ge. This might be evident at first sight because the energy of the latter is different from the additional states (compare Fig. 1). This argument neglects a possible change in the vacuum level which goes undetected in our measurements. For the sake of argument let us therefore assume that both defects have the same origin (dangling bond) and thus the same energy position with respect to the inner potential of a -Ge. Then it would be impossible to explain why dangling bonds that have been

removed by high-temperature hydrogenation can reappear upon RT hydrogenation unless RT hydrogenation etches away the healed surface, exposes virgin, that is, highly defective material, and proceeds from there with the hydrogenation. This scenario is untenable, however. We could imagine that only a few atomic layers of the material remain highly hydrogenated (mostly polyhydride configurations) and that the remaining unpassivated material gives rise to the observed defect band. (The hydrogen-rich surface shifts the vacuum level by changing the surface dipole layer down in energy so that the additional band appears at a different position compared to the unhydrogenated spectrum.) Then the disappearance of the defect band by the subsequent annealing would require an in-diffusion of hydrogen and at least a partial conversion of polyhydride configurations into monohydride, i.e., dangling-bond passivating configurations. This conversion has, to our knowledge, not been observed. In fact Lucovsky *et al.*²⁴ studied the evolution of the ir spectrum of GD a -Ge:H prepared at different temperatures. Modes due to Ge polyhydrides disappear rapidly above 200°C and are virtually annealed out at 300°C without any concomitant increase in the monohydride modes.

Hydrogen evolution has been studied in considerable detail (see, e.g., Beyer and Wagner²⁵) for a -Si:H and to a lesser extent in a -Ge:H.²⁶ In both cases two evolution maxima are observed. The lower one ($\sim 220^\circ\text{C}$ in a -Ge:H) is ascribed to the diffusion and evolution of H_2 from polyhydride configurations associated with inner surfaces; the high-temperature peak ($\sim 400^\circ\text{C}$ – 450°C in a -Ge:H) is due to hydrogen evolving from monohydride and the diffusing species is atomic hydrogen. These results preclude surface polyhydrides as a source of atomic hydrogen to passivate buried dangling-bond defects. This point is more directly illustrated in Fig. 7. The annealing at 200°C and 250°C does not change significantly the yield spectrum of $\sim 100 \text{ \AA}$ a -Ge evaporated on RT hy-

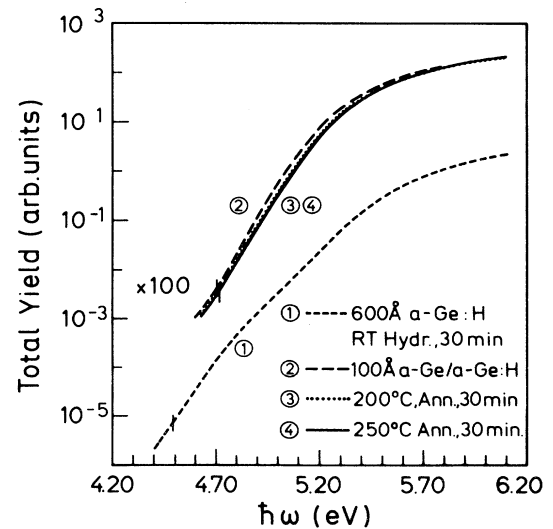


FIG. 7. Yield spectra of $\sim 100 \text{ \AA}$ a -Ge on RT hydrogenated a -Ge:H before and after annealing. Others are the same as in Fig. 1.

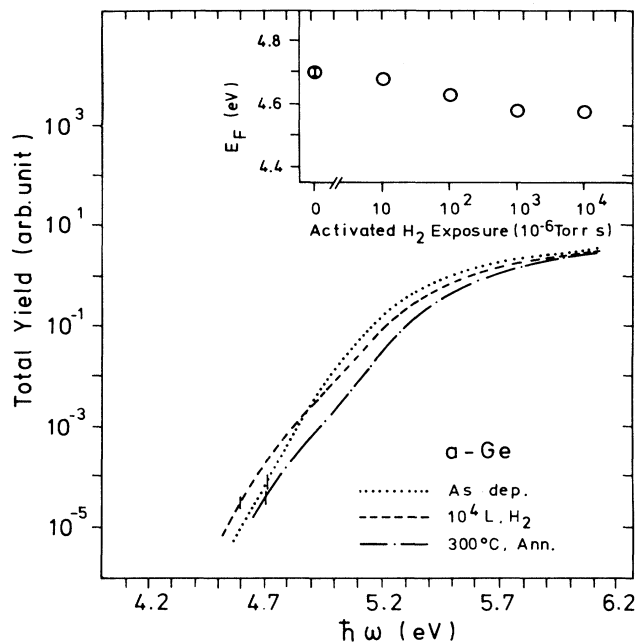


FIG. 8. Yield spectra of a -Ge exposed to activated H_2 . The inset shows the evolution of the Fermi energy with increasing activated hydrogen exposure.

drogenated a -Ge:H.

Further, Saxena *et al.*²⁷ remarked that the etching rate of a -Ge is about 100 times less than a -Si while the work of Shinar *et al.*²⁸ indicates comparable diffusion coefficients of H in a -Si:H and a -Ge:H.

It is conceivable that even the low-energy electron or ion bombardment of the a -Ge surface exposed to the plasma could introduce the deep defects that we observe in RT hydrogenated samples. To exclude this possibility we hydrogenated one sample by exposing it to atomic hydrogen obtained by the dissociation of H_2 at a hot ($T \sim 1800^\circ\text{C}$) W filament which was kept out of sight of the sample. Figure 8 shows the result which proves that the defect band and the concomitant shift in E_F is also produced under these circumstances albeit with a much reduced rate.

B. The nature of the polyhydride related defect

For high-temperature hydrogenation H diffuses into a -Ge, passivates dangling bonds (similar to the work²⁹ on a -Si), and reduces the concentration of weak strained bonds by insertion of two H atoms. These bring about a reduction in the defect band, a steeping of the valence-band tail, and a slight increase of the band gap compared to pure a -Ge. In low-temperature hydrogenation additional defects are produced due to an excess of hydrogen in the form of polyhydrides as argued above. Figure 9 is the Raman spectra of two a -Ge:H films hydrogenated at RT and 320°C , respectively. The bonded hydrogen concentration is about four times as much in the RT film as in the 320°C one. This is consistent with GD processes where more hydrogen can be incorporated by reducing

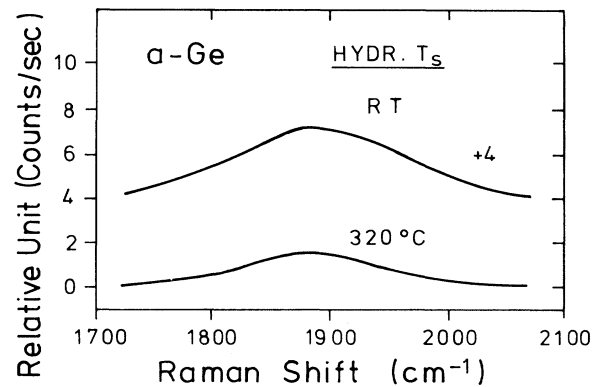


FIG. 9. Raman spectra of a -Ge:H on quartz substrate, hydrogenated at RT and 320°C for four hours. The spectra have been normalized using the intensities of TO vibration peaks.

the substrate temperature¹ as polyhydrides after the concentration of monohydrides saturates at 10–15 at.%.³⁰ The annealing of RT hydrogenated film can remove the defects by driving H out of polyhydride configurations [refer to similar work on GD a -Si:H (Ref. 4)]. Compared to high-temperature hydrogenation there is almost no additional recession of the valence-band edge for annealing.

Right now we still do not know the nature of the polyhydride related defect. It seems unlikely that any of the polyhydride configurations themselves, in which all bonds are satisfied, give rise to states in the gap. We could envisage, however, a bonding configuration that does produce the required midgap state and whose presence in sufficient quantity is favored by conditions that also favor the occurrence of polyhydride configurations. A possible candidate is the Ge-H-Ge three center bond. In its neutral state this configuration contains three electrons. According to the level scheme given by Fisch and Licciardello³¹ for the Si-H-Si equivalent two of them reside in a bonding orbital deep within the valence band whereas the third has to be placed in a nonbonding orbital that is likely to fall into the gap of a -Ge:H (Ref. 32) and would thus represent the observed defect in our spectra. The likelihood of such a three-center bond would increase with the hydrogen content c_H . It is as such linked to the low-temperature high c_H hydrogenation.

Bridging hydrogen has been observed by ir spectroscopy in amorphous hydrogenated III-V compounds (GaP, GaAs, GaSb) (Ref. 33) as very broad bands (several hundred cm^{-1}) around 1500 cm^{-1} . Assuming that in a -Ge:H (and for that matter also in a -Si:H) hydrogenated at RT the hydrogen content in the sampling depth of our method ($\sim 50 \text{ \AA}$) approaches the bulk hydrogen concentration of RT GD a -Ge:H/ a -Si:H,²⁴ namely, $\sim 10^{22} \text{ cm}^{-3}$, it is evident that the defect producing Ge-H-Ge configurations ($\sim 10^{18} \text{ cm}^{-3}$) constitute only a small (10^{-4}) minority of hydrogen configurations that will not be detected by ir spectroscopy.

C. Implication for defects in GD films

What are the implications of these findings for GD a -Si:H and a -Ge:H? First, we notice that the concentration

of the defect ($\sim 10^{18} \text{ cm}^{-3}$) measured for RT hydrogenated *a*-Ge is comparable in magnitude to that found in GD *a*-Si:H and *a*-Ge:H prepared at RT. In both cases the high defect density is associated with a high hydrogen concentration ($\sim 30 \text{ at. } \%$) present in the form of polyhydrides.

After annealing to $\sim 200^\circ\text{C}$ – 250°C the bulk hydrogen concentration and with it the high defect density is reduced to the “optimal” values of 5–10 at. % and 10^{15} – 10^{16} cm^{-3} , respectively. A similar decrease in hydrogen content and defect density is observed in our samples at higher temperature: $\sim 300^\circ\text{C}$. This fact is in keeping with the higher stability of polyhydride configurations at the surface. Photoemission results on GD *a*-Si:H and *a*-Ge:H (Ref. 10) with a similar surface sensitivity as the one achieved here indicate predominantly dihydride and trihydride configurations at temperatures when these configurations are absent in the bulk of the material as confirmed by ir measurements. The same conclusion was drawn by Sasaki *et al.*¹⁴ from electron-energy-loss spectra on *a*-Si_{1-x}Ge_x:H alloys.

This leads us to an answer to the question raised in the introduction, namely, the high-surface defect density in GD *a*-Si:H films grown at optimal temperature. We maintain that this defect density which was estimated by Curtins and Favre⁹ to be $\sim 10^{18} \text{ cm}^{-3}$ is directly related to the polyhydride configurations at the surface as seen in photoemission. This defect density is therefore not surprisingly exactly the concentration of near surface defects deduced from yield spectra of GD *a*-Si:H prepared under optimum conditions.¹² Furthermore, the fact that these defects in GD *a*-Si:H ($T_s = 250^\circ\text{C}$) are *not* reduced by post-deposition hydrogenation confirms that they cannot be regarded as due to conventional dangling bonds which would be passivated by extra hydrogen atoms brought to the surface.¹²

Hata *et al.*¹⁵ have recently modeled the relationship between defect density and film thickness in GD *a*-Si:H for thicknesses covering four orders of magnitude. Their model is based on the assumption that deposited material at the growing surface has a high defect density that anneals out during the course of the deposition in such a way that a gradient in defect density is maintained. The defect density measured by an integrating method such as PDS is therefore an average over this defect profile which depends on film thickness and on annealing rates. The authors were able to model their data with a surface defect density of $4 \times 10^{17} \text{ cm}^{-3}$ and a thermally activated annealing rate with an average activation energy of 1.05 eV.

A microscopic interpretation of these data in light of our results would be the following. The surface of the growing film maintains a high concentration of hydrogen as a result of the plasma surface reactions which deposit material mainly in the form of SiH_x ($x = 1, 2, 3$).⁷ This hydrogen-rich region provides also the high defect density in the form of Si-H-Si configurations which account for only about 10^{-4} of the bonded hydrogen content. The annealing of these defects is brought about by hydrogen elimination and outdiffusion. The activation energy

of 1.05 eV for the annealing process as used by Hata *et al.*¹⁵ was taken from Ref. 34. Higher activation energies for the annealing of defects (1.6 eV) have been reported.⁶ In this case the diffusion of atomic hydrogen is considered the rate limiting step which has activation energies in the range of 1.2 to 1.6 eV,³⁵ i.e., somewhat higher than 1.05 eV in Ref. 15.

As a matter of fact, it is not clear how sensitive the model of Ref. 15 depends on the exact value of the activation energy. Instead of the diffusion of atomic hydrogen one might consider the outdiffusion of H₂ through the ill connected hydrogen-rich surface layer as a means for the system to lower its hydrogen content and thereby the hydrogen-induced defects. In this case the diffusion is not the rate limiting step but rather the formation of H₂.²⁵ Considerations along these lines were made by Hundhausen *et al.*³⁶ to explain the conspicuous hydrogen depletion or accumulation at GD *a*-Si:H interfaces of different doping levels that occur in doping modulated superlattices.

An unresolved issue is the *g* value of the defect proposed here. The dangling-bond defect in *a*-Si has a *g* factor⁷ of 2.0055. The *g* value for the defects in GD *a*-Si:H prepared at RT is quoted as 2.0050 by Yamasaki *et al.*³⁷ While it is not obvious that this lowering is significant in terms of the experimental uncertainty it is worth mentioning that the magnetically active defect in polymerlike *a*-Si:H has a *g* value of 2.0043.³⁸

V. SUMMARY AND CONCLUSIONS

We have investigated the occupied density of gap states in *a*-Ge as a function of hydrogenation at various temperatures and for different annealing steps. The results indicate that a hydrogen-related defect level 0.45 eV above the valence-band maximum occurs in RT hydrogenated samples. It is distinguishable from the dangling-bond defects in unhydrogenated *a*-Ge on account of its energy and annealing behavior.

We argue that this type of defect is responsible for the extra surface defect density found in GD *a*-Ge:H and *a*-Si:H films prepared so as to have the lowest possible bulk defect density. With this defect the growth temperature and thickness-dependent average defect density in GD films can be explained.

Because all evidence points towards a direct involvement of hydrogen in the defect we tentatively attribute it to a Ge-H-Ge or Si-H-Si three-center bond. In its neutral state a single electron resides in a nonbonding orbital which accounts for the paramagnetic nature of the defect and an energy likely to be close to midgap.

ACKNOWLEDGMENTS

The authors would like to thank A. Akihiko, H. Rose, and A. Dittrich for their experimental assistance. S.J. acknowledges support by the Max Planck Society. This work was supported in part by the Bundesminister für Forschung und Technologie under Contract No. 0328962A.

- *Present address: Department of Physics, Boston University, 590 Commonwealth Ave., Boston, MA 02215.
- ¹J. C. Knights, G. Lucovsky, and R. J. Nemanich, *J. Non-Cryst. Solids* **32**, 393 (1979).
 - ²G. A. N. Connell and J. R. Pawlik, *Phys. Rev.* **13**, 787 (1976).
 - ³H. Fritzsche, C. C. Tsai, and P. Persans, *Solid State Technology* **21**, 55 (1978).
 - ⁴D. K. Biegelsen, R. A. Street, C. C. Tsai, and J. C. Knights, *Phys. Rev. B* **20**, 4839 (1979).
 - ⁵T. D. Moustakas, D. A. Anderson, and W. Paul, *Solid State Commun.* **23**, 155 (1977).
 - ⁶G. D. Parsons, C. Wang, M. J. Williams, and G. Lucovsky, *J. Non-Cryst. Solids* **114**, 178 (1989).
 - ⁷B. A. Scott, J. A. Reimer, and P. A. Longeway, *J. Appl. Phys.* **54**, 6853 (1983).
 - ⁸D. G. Ast and M. H. Brodsky, *J. Non-Cryst. Solids* **35/36**, 611 (1980); *Philos. Mag. B* **41**, 273 (1980).
 - ⁹H. Curtains and M. Favre, in *Advances in Amorphous Silicon and Related Materials*, edited by H. Fritzsche (World Scientific, Singapore, 1988), p. 329.
 - ¹⁰L. Ley, in *Semiconductors and Semimetals*, edited by J. I. Pankove (Academic, Orlando, 1984), Vol. 21B, p. 385.
 - ¹¹L. Yang, B. Abeles, W. Eberhardt, H. Stasiewski, and D. Sondericker, *Phys. Rev. B* **39**, 3801 (1989).
 - ¹²K. Winer and L. Ley, in Ref. 9, p. 365.
 - ¹³S. Aljishi, S. Jin, and L. Ley, in *Amorphous Silicon Technology*, edited by A. Madan, M. Thompson, P. C. Taylor, Y. Hamakawa, and P. G. LeComber, MRS Symposia Proceedings No. 149 (Materials Research Society, Pittsburgh, 1989), p. 125.
 - ¹⁴H. Sasaki, M. Deguchi, K. Sate, and M. Aiga, *J. Non-Cryst. Solids* **114**, 672 (1989).
 - ¹⁵N. Hata, S. Wagner, P. Roca i Cabarrocas, and M. Favre (unpublished).
 - ¹⁶J. Kakalios and W. Jackson, in Ref. 9, p. 272.
 - ¹⁷D. Kaplan, N. Sol, G. Velasco, and P. A. Thomas, *Appl. Phys. Lett.* **33**, 440 (1978); P. A. Thomas and J. C. Flachet, *Philos. Mag. B* **51**, 55 (1985).
 - ¹⁸W. Thompson, *Philos. Mag.* **46**, 82 (1898).
 - ¹⁹R. H. Fowler, *Phys. Rev.* **38**, 45 (1931).
 - ²⁰W. B. Jackson, S. M. Kelso, C. C. Tsai, J. W. Allen, and S.-J. Oh, *Phys. Rev. B* **31**, 5187 (1985).
 - ²¹C. G. Ribbing, D. T. Pierce, and W. E. Spicer, *Phys. Rev. B* **4**, 4417 (1971).
 - ²²M. L. Theye, A. Gheorghiu, K. Driss-Khodja, and C. Boccara, *J. Non-Cryst. Solids* **77/78**, 1293 (1985).
 - ²³K. L. Gruntz, L. Ley, M. Cardona, R. Johnson, G. Harbeke, and B. von Roedern, *J. Non-Cryst. Solids* **35/36**, 453 (1980).
 - ²⁴G. Lucovsky, S. S. Chao, J. Yang, J. E. Tyler, R. C. Ross, and W. Czubatytj, *Phys. Rev. B* **31**, 2190 (1985).
 - ²⁵W. Beyer and H. Wagner, *J. Non-Cryst. Solids* **59/60**, 161 (1983).
 - ²⁶D. Martin, B. Schroeder, M. Leidner, and H. Oechsner, *J. Non-Cryst. Solids* **114**, 537 (1989).
 - ²⁷N. Saxena, D. E. Albright, C. M. Fortmann, T. W. F. Russell, P. M. Fauchet, and I. H. Campbell, *J. Non-Cryst. Solids* **114**, 801 (1989).
 - ²⁸R. Shinar, S. Mitra, X. L. Wu, and J. Shinar, *J. Non-Cryst. Solids* **114**, 220 (1989).
 - ²⁹W. B. Jackson, C. C. Tsai, and R. Thompson, *Phys. Rev. Lett.* **64**, 56 (1990).
 - ³⁰G. Lucovsky, B. N. Davidson, G. N. Darsons, and C. Wang, *J. Non-Cryst. Solids* **114**, 154 (1989).
 - ³¹R. Fisch and D. C. Licciardello, *Phys. Rev. Lett.* **41**, 889 (1978).
 - ³²In the work of Ref. 31 the Si-H-Si three-center bond forms a defect with a negative correlation energy U . In our opinion on the case a positive U defect which would give rise to an ESR signal is just as convincing.
 - ³³Z. P. Wang, L. Ley, and M. Cardona, *Physica B+C* **117/118B**, 968 (1983).
 - ³⁴Z. E. Smith and S. Wagner, *Phys. Rev. B* **32**, 5510 (1985).
 - ³⁵W. Beyer, J. Herion, and H. Wagner, *J. Non-Cryst. Solids* **114**, 217 (1989).
 - ³⁶M. Hundhausen, P. V. Santos, L. Ley, F. Habraken, W. Beyer, R. Primig, and G. Gorges, *J. Appl. Phys.* **61**, 556 (1987).
 - ³⁷S. Yamasaki, S. Kuroda, H. Okushi, and K. Tanaka, *J. Non-Cryst. Solids* **77/78**, 339 (1985).
 - ³⁸S. Nonomura, S. Hattori, H. Hayashi, T. Itoh, and S. Nitta, *J. Non-Cryst. Solids* **114**, 729 (1989).